Beam-Induced Heating: A Review and Summary

Hugo Alistair Day, Olav Berrig, Fritz Caspers,
Alexej Grudiev, Elias Metral, Nicolas Mounet,
Benoit Salvant

January 30, 2013

Abstract

A review of the first two years of study are presented. These topics consist of; Simulations of coaxial wire measurements of the impedance of asymmetric devices, coaxial wire measurements of ferrite kicker magnets for use in the SPS and LHC and impedance studies of a number of potential collimator upgrades for the LHC, focusing on the phase 2 secondary collimators for the LHC. Also disucssed is future work towards completion of the PhD and a timetable of writing to ensure timely completion.

Contents

0.1 Introduction

The concept of beam power loss due to interaction with machine impedance has been understood for some time [cite chao/Ng for parasitic loss]. This has two effects - the neccessity of compensating for this with the machines RF systems and also the heating of the surrounding equipment by the lost energy. This is especially a concern with high beam current machines, which may experience signficant heat loads due to large longitudinal impedances. This has previously been observed in both electron [Mauro presentation for PEPII] and hadron machines [LHC Mini-Cham, Evian, Chamonix] and continues to be a active concern for high current machines.

In this note is derived the fundamental relationship between the longitudinal beam parameters and longitudinal beam coupling impedance and the power lost by a particle beam. The effect of different beam parameters is then investigated, and simple relationships derived to explain how they change the power lost by a beam. Finally the effect of the longitudinal beam profile is demonstrated to emphasise how drastic the effect of longitudinal profile can have on the power loss calculations.

0.2 Defining and Deriving Power Loss in Circular Accelerators

Defining and Deriving Power Loss in Circular Accelerators

When a charged particle interacts with a wakefield it's energy changes due to the field that it sees. Assuming a beam with a longitudinal distribution $\rho(\tau)$, normalised such that $\int d\tau\rho(\tau) = I_b$. Now a normalised longitudinal distribution ρ_n is introduced, such that $\rho = N_b f_0 e \int d\tau\rho_n$. Thus the energy change of the distribution ρ traversing a pipe for a distance L is given by [**?**, **?**]

$$\Delta E = -\left(f_0 e N_b\right)^2 \int_{-\infty}^{\infty} d\tau^{'} \rho_n\left(\tau^{'}\right) \int_{-\infty}^{\infty} d\tau \rho_n\left(\tau\right) W_{\parallel}\left(\tau^{'} - \tau\right). \tag{1}$$

Written in terms of the Fourier transformed quantities this becomes

$$\Delta E = \frac{-1}{2\pi}\left(f_0 e N_b\right)^2 \int_{-\infty}^{\infty} d\omega \left|\lambda\left(\omega\right)\right|^2 \Re e\left[Z_{\parallel}\left(\omega\right)\right] \tag{2}$$

where

$$\lambda\left(\omega\right) = \frac{1}{\sqrt{2\pi}} \int_{-\infty}^{\infty} d\tau \rho_n\left(\tau\right) e^{j\omega\tau}. \tag{3}$$

For a mode expansion representation of the wakefunction as a sum of loss factors, the total energy change can be written as

$$\Delta E = \left(f_0 e N_b\right)^2 \sum_{n=0}^{\infty} k_n \left|\lambda\left(\omega_n\right)\right|^2. \tag{4}$$

These terms are valid only for a single pass of the beam through the impedance (i.e. for a linear accelerator). In the case where the beam traverse the same impedance multiple times (i.e. a circular accelerator) it is necessary to take into account the wakefields induced by previous traversals. In this case the energy lost by the beam due to traversing the pipe is given by

$$\Delta E = -\left(f_0 e N_b\right)^2 \int_{-\infty}^{\infty} d\tau^{'} \rho_n\left(\tau^{'}\right) \int_{-\infty}^{\infty} d\tau \rho_n\left(\tau\right) \sum_{q=0}^{\infty} W_{\parallel,q}\left(q\frac{C}{c} + \tau^{'} - \tau\right) \tag{5}$$

where C is the circumference and q sums over revolutions. In general impedance is the more useful property to use compared to wakefields. Using the Poisson sum formalism and the following identity

$$\sum_{n=-\infty}^{\infty} F\left(na\right) = \frac{1}{a} \sum_{p=-\infty}^{\infty} \tilde{F}\left(\frac{2\pi p}{a}\right) \tag{6}$$

where $F(\tau)$ and $\tilde{F}(\omega)$ are arbitary Fourier transformed pairs. This relationsgip shows that summing a function at regular intervals a is equal to summing over its Fourier transformed counterpart at regular intervals $\frac{2\pi}{a}$. In particular a useful special case is

$$\sum_{n=-\infty}^{\infty} e^{-j\omega\tau} = 2\pi \sum_{p=-\infty}^{\infty} \delta\left(x - 2\pi p\right). \tag{7}$$

Thus for the total impedance over the accelerator $Z_{\parallel}$ the energy loss is

$$\Delta E = -\frac{\omega_0}{2\pi} \left(f_0 e N_b\right)^2 \sum_{n=-\infty}^{\infty} \left|\lambda\left(p\omega_0\right)\right|^2 \Re e\left[Z_{\parallel}\left(p\omega_0\right)\right]. \tag{8}$$

To find the power the power loss of the bunch distribution it is simply necessary to normalise by the revolution frequency. In addition we use the property of the longitudinal impedance that

$$\Re e\left[Z_{\parallel}\left(\omega\right)\right] = \Re e\left[Z_{\parallel}\left(-\omega\right)\right] \tag{9}$$

to give the power lost by a single bunch in a circular accelerator as

$$P_{loss,single} = -2\left(f_0 e N_b\right)^2 \sum_{n=-\infty}^{\infty} \left|\lambda\left(p\omega_0\right)\right|^2 \Re e\left[Z_{\parallel}\left(p\omega_0\right)\right]. \tag{10}$$

To consider the case of more than one bunch in a circular machine, it is possible to consider Eqn. 5, but in this case assume a time difference between the successive summed wakes as $\frac{C}{n_{bunch}c}$, in this case assuming that the bunches are equally space around the machine, giving the energy loss for one bunch in a machine with n_{bunch} is

$$\Delta E_{bunches} = -\left(f_0 e N_b\right)^2 \int_{-\infty}^{\infty} d\tau^{'} \rho_n\left(\tau^{'}\right) \int_{-\infty}^{\infty} d\tau\, \rho_n\left(\tau\right) \sum_{q=0}^{\infty} W_{\parallel,q}\left(q\frac{C}{n_{bunch}c} + \tau^{'} - \tau\right). \tag{11}$$

Following the previous derivation this leads to a power loss due to a single bunch in a train of

$$P_{loss,sbt} = -2n_{bunch}\left(f_0 e N_b\right)^2 \sum_{n=-\infty}^{\infty} \left|\lambda\left(pn_{bunch}\omega_0\right)\right|^2 \Re e\left[Z_{\parallel}\left(pn_{bunch}\omega_0\right)\right]. \tag{12}$$

Subsequently taking the sum over all n_{bunch} produces the total power loss

$$P_{loss} = -2\left(f_0 e n_{bunch} N_b\right)^2 \sum_{n=-\infty}^{\infty} \left|\lambda\left(pn_{bunch}\omega_0\right)\right|^2 \Re e\left[Z_{\parallel}\left(pn_{bunch}\omega_0\right)\right]. \tag{13}$$

If the wakefield effectively decays to zero in less than the distance between two succeeding bunches, then this is simply equivalent to an integral. This indicates that for sharp resonant impedances that last over multiple bunch intervals/turns of the machine, only the sum formalism is valid.

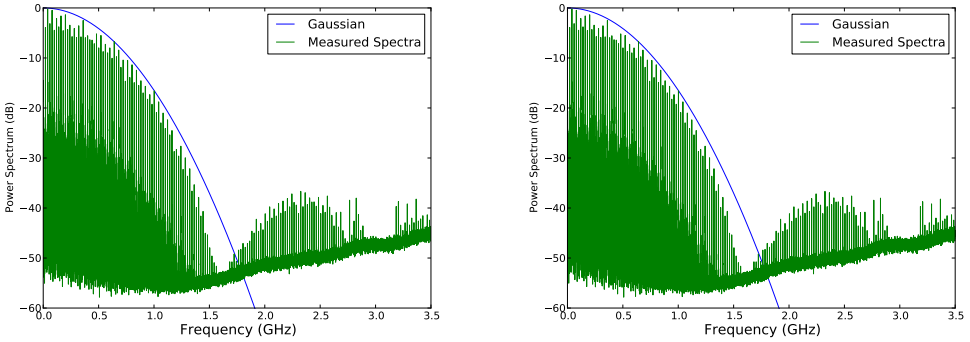

(a) (b)

Figure 1: A comparison of 1(a) a measured beam power spectrum and a gaussian bunch of the same bunch length in the frequency domain and 1(b) the resulting time domain beam profile. The gaussian has a bunch length ($4\sigma_z$ = 1.2ns)

0.3 Longitudinal Beam Profiles

As shown by the derivations in Section 0.2, asides from the longitudinal impedance of the device under consideration the longitudinal profile of the circulating bunches also contributes to the power loss in the machine. In past works it has generally been assumed that bunches in accelerators have a Gaussian profile [ref Sacherer/Grudiev/Laclare](seen in Eqn. 14, where $4\sigma_z = t_b$, t_b is the bunch length) when approaching the analytical treatment of beam instabilities, both single-bunch and multi-bunch. Recent measurements of the power spectrum of particle beams, especially in the LHC [ref theo/phillipe] have shown characteristics that the Gaussian profile does not predict, for example the high frequency secondary peak as seen in Fig. 1. To make more realistic predictions of heat loss due to beam impedance in the machine it is thus necessary to find bunch profiles which reproduce this behaviour.

$$\lambda(t) = e^{\frac{-t^2}{2\sigma^2}} \tag{14}$$

A number of different longitudinal bunch profiles have been investigated in the past. Here we shall look at 3 other bunch profiles; a parabolic line density (see Eqn. 15), $\cos^2$ (see Eqn. 16), water-bag (see Eqn. 17).

$$A(t) = \int_{-\infty}^{\infty} \lambda(\omega)\, e^{j\omega t} d\omega = \begin{cases} 1 - \left(\frac{2t}{t_b}\right)^2 & \text{if } |t/2| \leq t_b \\ 0 & \text{if } |t/2| > t_b \end{cases} \tag{15}$$

$$A(t) = \int_{-\infty}^{\infty} \lambda(\omega)\, e^{j\omega t} d\omega = \begin{cases} cos^2\left(\frac{\pi t}{t_b}\right) & \text{if } |t/2| \leq t_b \\ 0 & \text{if } |t/2| > t_b \end{cases} \tag{16}$$

$$A(t) = \int_{-\infty}^{\infty} \lambda(\omega)\, e^{j\omega t} d\omega = \begin{cases} \sqrt{1 - \left(\frac{2t}{t_b}\right)^2} & \text{if } |t/2| \leq t_b \\ 0 & \text{if } |t/2| > t_b \end{cases} \tag{17}$$

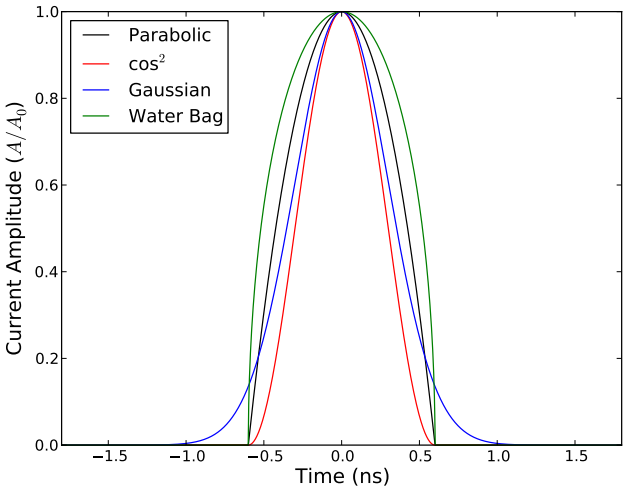

Figure 2: The longitudinal bunch profile of a number of bunch distributions. Note that all of them are normalised to have a peak bunch current of 1. For the gaussian distribution the bunch length is the 4σ value. The bunch length $\tau_b = 1.2ns$

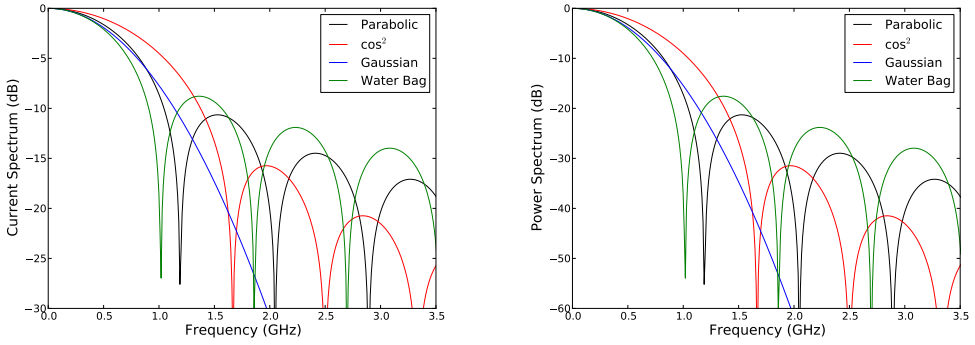

(a) (b)

Figure 3: The frequency domain 3(a) current spectrum and 3(b) power spectrum for a number of different bunch profiles with a bunch length $\tau_b = 1.2ns$.

The comparison of these bunch profiles in the time domain are shown in Fig. 0.3. Note all bunch currents are normalised to their peak value. The corresponding current and power spectrums are shown in Fig. 0.3. There are several things to note about these spectra; firstly that the non-infinite distribution of the non-gaussian bunch profiles gives rise to a number of high frequency lobes in the power spectrum, and secondly the interval of these nodes depends heavily on the bunch profile.

To illustrate more clearly the effect of changing the bunch length on the power spectrum, a number of bunch profiles and the corresponding power spectra with different bunch lengths are shown below. Firstly, consider a gaussian bunch profile. It can be seen in Fig. 4 that by increasing the bunch length that the magnitude at high frequencies is decreased quite substantially as the bunch length increases. If we consider a finite

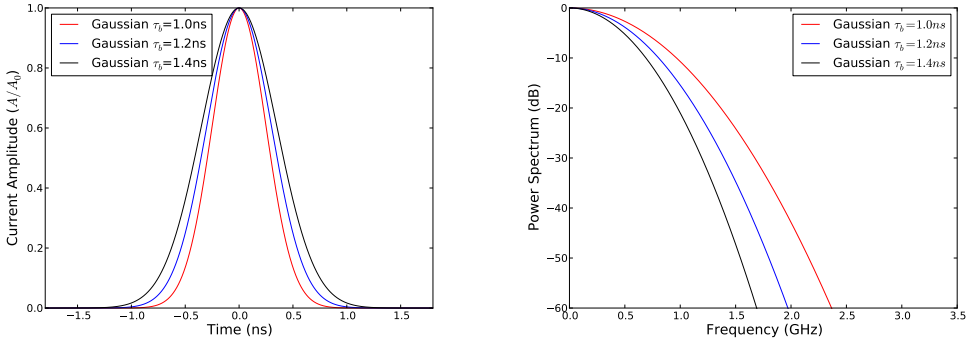

(a) (b)

Figure 4: 4(a) The longitudinal profile and the 4(b) associated bunch power spectrum for a number of bunch lengths assuming a gaussian bunch profile.

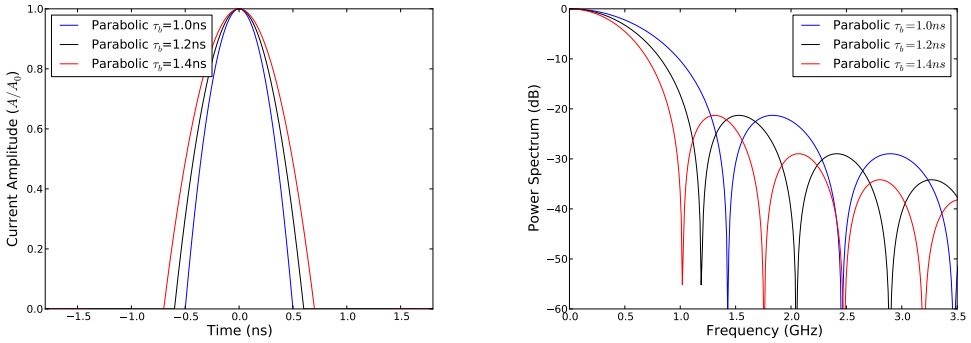

(a) (b)

Figure 5: 5(a) The longitudinal profile and the 5(b) associated bunch power spectrum for a number of bunch lengths assuming a parabolic bunch profile.

bunch profile (non-gaussian), we note that we have high frequency lobes. The peak frequency of these lobes depends on the bunch length, as illustrated using a parabolic bunch profile for bunch lengths $\tau_b = 1ns, 1.2ns, 1.4ns$ in Fig. 0.6.1. As the bunch length is increased the lobes move to lower frequencies, and the width of the first branch decreases, as seen for the gaussian bunch. Similar behaviour is observed with the $\cos^2$ and water-bag bunch profiles.

Finally, a comparison of a measured bunch power spectra and the analytical power spectra is shown in Fig. 0.3. It can be seen that whilst it is possible to replicate some of the properties of the measured spectrum, an exact replication is non-trivial. Further investigation into the appropriate bunch profile is ongoing.

0.4 Beam induced heating due to a low Q impedance

For an impedance with a characteristic Q that is small (Q $<$ 10), it can be seen that the impedance peak will interact substantially with a number of beam harmonics (see

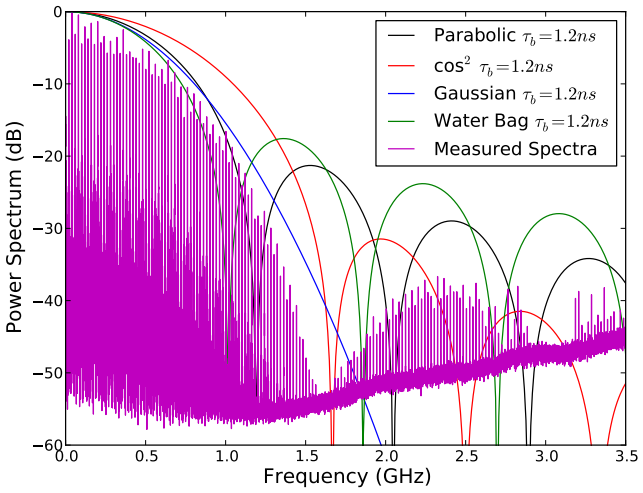

Figure 6: A comparison of a measured beam power spectrum and a number of analytical bunch profiles assuming a bunch length of 1.2ns.

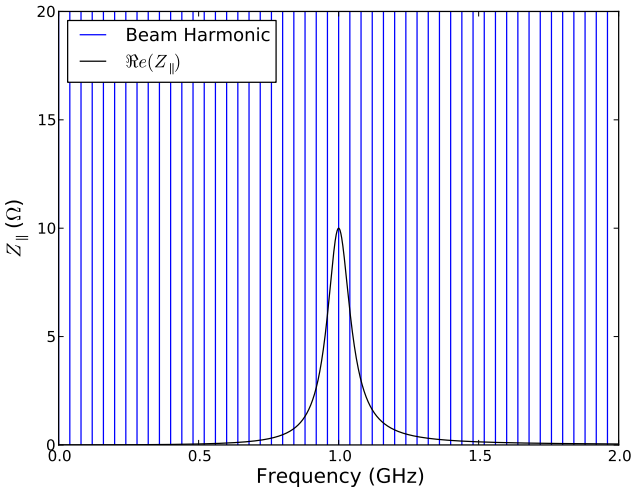

Figure 7: The beam harmonics of a beam with a bunch spacing of 25ns overlayed on the real component of the longitudinal impedance an example of a low Q impedance ($R_s = 10\omega$, Q = 10, $f_{res} = 1GHz$). The blue lines represent the frequency of a beam harmonic, not necessarily the magnitude of the power spectrum at that point. Note that a number of beam harmonics overlay non-zero impedance values.

Fig. 0.4) due to the broad frequency range it occupies.

Further investigation of the longitudinal beam spectrum reveals that there is significant structure between the major harmonics (which are due to the bunch spacing of the beam) which can be attributed to the other time structures of the beam, for example the bunch train spacing, or the interval between the pilot bunch train and the subsequent

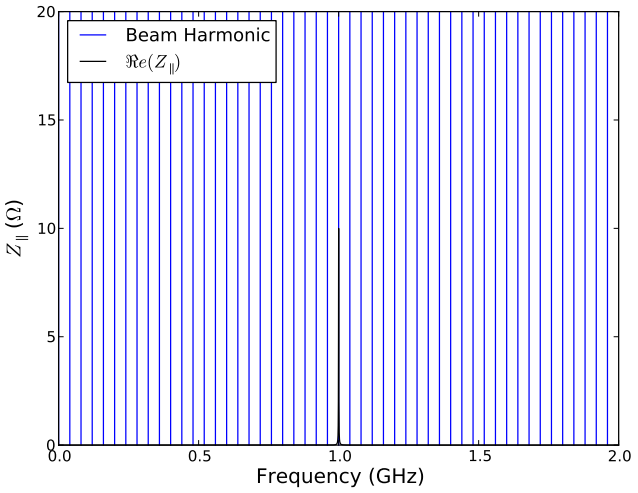

Figure 8: The beam harmonics of a beam with a bunch spacing of 25ns overlayed on the real component of the longitudinal impedance an example of a high Q impedance ($R_s = 10\omega$, Q = 1000, $f_{res} = 1GHz$). The blue lines represent the frequency of a beam harmonic, not necessarily the magnitude of the power spectrum at that point. Note that only a single beam harmonic overlays a non-zero impedance values.

bunch train. As such the treatment of the estimation of beam losses requires a broad spectrum approach. If we consider Eqn.**??** we see that we can treat the power losses in an integral form. We can observe a number of properties using this assumption. The power loss is proportional to the beam properties in the following manner:

1. $P_{loss} \propto N^2$
2. $P_{loss} \propto n_{bunch}$

0.5 Beam induced heating due to a high Q impedance

In contrast to the overlap of the beam spectrum with a low Q impedance, for a high Q impedance only one beam harmonic lies upon the resulting impedance to any significant quantity. This is illustrated in Fig 0.5 If we consider Eqn 13 and consider the situation where

$$\left(2\left|\lambda\left(p\omega_{rev}n_{bunch}\right)\right|^2\Re e\left(Z_\parallel\left(p\omega_{rev}n_{bunch}\right)\right)\right) = \begin{cases}\left(2\left|\lambda\left(\omega_{res}\right)\right|^2\Re e\left(Z_\parallel\left(\omega_{res}\right)\right)\right) & \text{if } p\omega_{rev}n_{bunch} = \omega_{res} \\ 0 & \text{if } p\omega_{rev}n_{bunch} != \omega_{res}\end{cases} \tag{18}$$

It can then be seen that Eqn 13 simplifies to

$$P_{loss} = \left(\omega_{rev}eN_bn_{bunch}\right)^2\left(2\left|\lambda\left(\omega_{res}\right)\right|^2\Re e\left(Z_\parallel\left(\omega_{res}\right)\right)\right). \tag{19}$$

The following properties can subsequently be seen as a result:

1. $P_{loss} \propto N^2$
2. $P_{loss} \propto n_{bunch}^2$, provided that the resonant frequency of the resonance continues to coincide with a beam harmonic.

0.6 Some Examples of the Beam-Induced Heating

In this section we shall illustrate some important factors that have been covered in previous sections. In particular, the interaction of different bunch profiles at different bunch lengths with an example cavity resonance will be covered in some detail to illustrate how the estimated heating can change drastically depending on higher frequency lobes in the beam current spectrum. In addition, the heating due to two particle beams in the same vacuum chamber shall be briefly covered for interest.

0.6.1 The Effect of Bunch Length on Power Loss

As can be seen in Figs. 0.3 and , the bunch profile and the bunch length can significantly alter the magnitude of the beam current at higher frequencies. To illustrate this, let us consider two resonant impedances, one broadband Z_{bb} and one narrow band Z_{nb} impedance, characterised by having a low-Q and a high-Q respectively. Both impedances shall have the same resonant shunt impedance $R_s = 100\Omega$. The broadband impedance shall have a $Q_{bb} = 1$, and the narrow band impedance $Q_{nb} = 1000$. The resonant frequency will be changed to illustrate effects in different regimes of the bunch length and of different bunch profiles.

We shall use the gaussian bunch profile and the cos^2 bunch profile for these examples. The gaussian is useful to illustrate the effect of just the changing bunch length, and the cos^2 due to the presence of a high frequency lobe in it's frequency domain current spectrum. The cos^2 frequency domain current profile is given by

$$I(\omega) = \frac{sin(\omega\tau_b/2)}{\omega\tau_b/2\left[1-(\omega\tau_b/2)^2\right]}. \tag{20}$$

First we shall consider a narrowband impedance which has a resonant frequency $\omega_0 = 2GHz$ which falls upon a beam harmonic such that $\omega_0 = n\omega_{rev}$ where n is an integer. It should be noted that for other cases the contribution of these sources of heating is negligible due to the small beam current at this frequency. There are two extreme cases; that of $\omega_0 \gg 1/\tau_b$, in which it can be seen that the current spectrum will be negligible at the frequency of the impedance, and $\omega_0 \ll 1/\tau_b$ where the beam current spectrum is essentially the same as the DC spectral component. The transition in this intervening regime is shown in Fig 0.6.1, assuming a bunch current of 1A. It can be seen that in this case the heating falls drastically as the bunch length increases.

If we instead consider a $\cos^2$ distribution we instead see the effect of the secondary lobes in the beam current spectrum. The power loss with bunch length is shown in Fig. **??** in comparison to that of the gaussian profile. The beam power spectrum for

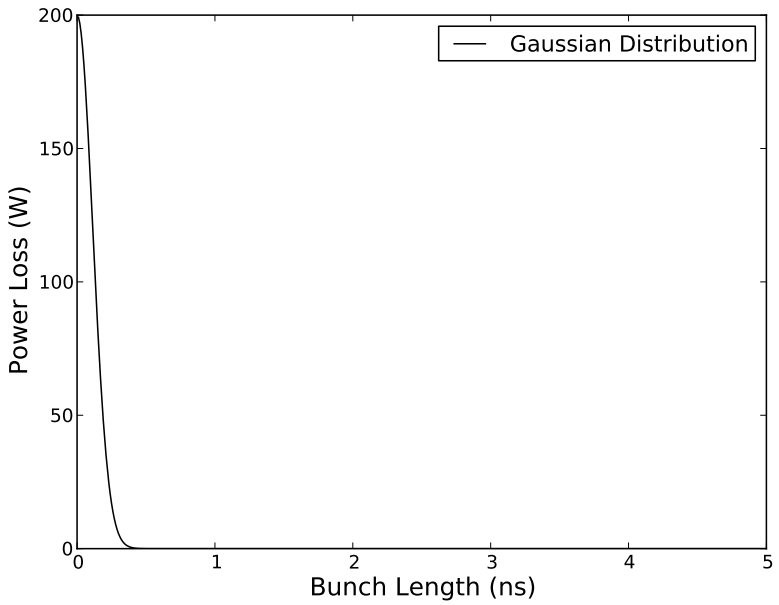

Figure 9: The change in power loss due to a narrow band resonance characterised by $\omega_0 = 2GHz$, $R_s = 100\Omega$, $Q = 1000$ with a gaussian bunch distrbution of different lengths.

a number of different bunch lengths are shown with the real component of the longitudinal impedance in Fig. 10(b). Here it can be clearly seen that the intersection of the secondary lobe with the resonant impedance causes a peak in the power lost by the beam, highlighting the neccessity to be aware of the resonant frequencies of resonant impedances with relation to the beam harmonics.

For the broadband heating we shall consider a resonant impedance defined by the following parameters, $\omega_0 = 2GHz$, $Q = 1$, $R_s = 100\Omega$. To account for the multiple beam harmonics that will interact with the resonance, it is assumed that the beam harmonics in this case occur at 20MHz intervals. The impedance and the beam power spectrum is shown in Fig. 11(a) and the resulting power loss in Fig. 11(b) where it can be seen that the power loss decreases slowly with increasing bunch length. This is due to the significant contribution to the power loss at low frequencies, in which the component of the beam power spectrum decreases only marginally due to the decreasing bunch length.

0.6.2 Beam-Induced Heating due to two traversing beams

Previous work [cite A. Grudiev TCTVB/TCLIA] has investigated the effect of two beams in a vacuum on the beam-induced heating. This is restated here for the sake of completeness.

To begin, consider the two currents $I_{b1} = I_0 e^{i\phi_1}$ and $I_{b1} = -I_0 e^{i\phi_2}$ representing two counter rotating beams. I_0 represents the beam current, and $\phi_{1/2}$ the phase of beam 1

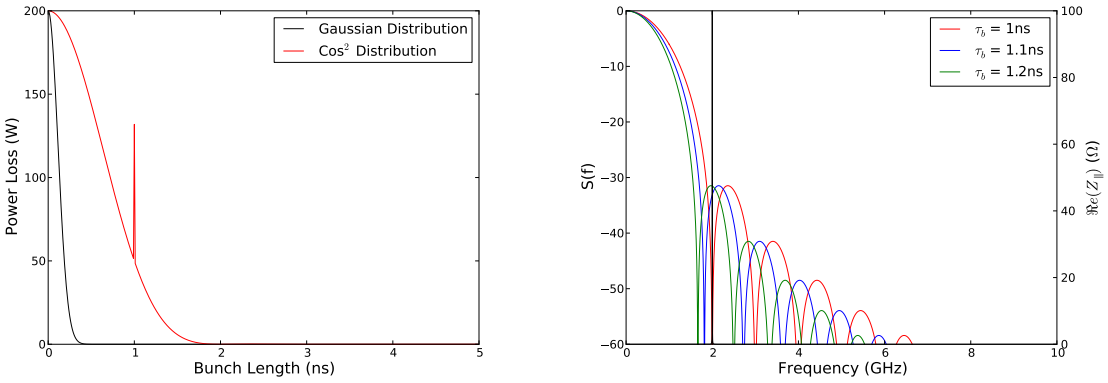

(a) (b)

Figure 10: 10(a) The change in power loss due to a narrow band resonance characterised by $\omega_0 = 2GHz$, $R_s = 100\Omega$, $Q = 1000$ interacting with a $\cos^2$ bunch distribution with different bunch lengths. The impedance and the beam power spectrum are shown in 10(b) to illustrate how this relates to the power loss.

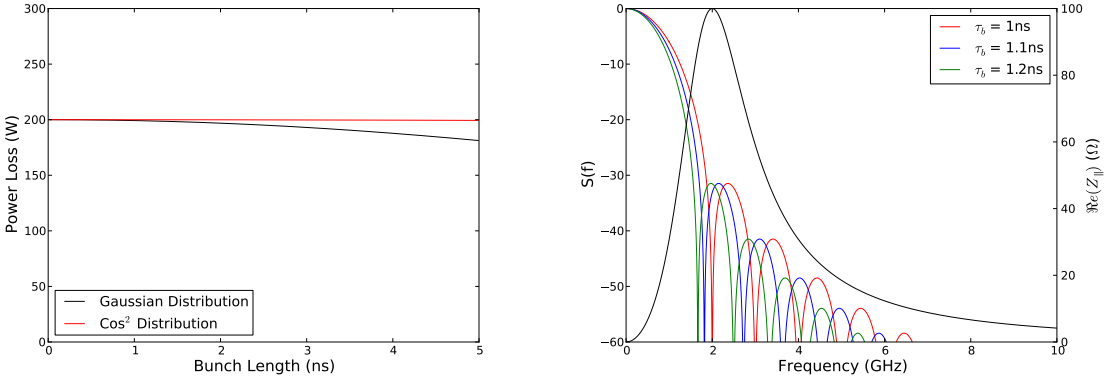

(a) (b)

Figure 11: 11(a) The change in power loss due to a narrow band resonance characterised by $\omega_0 = 2GHz$, $R_s = 100\Omega$, $Q = 1$ interacting with a $\cos^2$ bunch distribution with different bunch lengths. The impedance and the beam power spectrum are shown in 11(b) to illustrate how this relates to the power loss.

and beam 2 respectively. Each beam also sees a seperate potential when it traverses the impedance, given by $V_{b1} = \int_{b1} E_z e^{i\omega_0 z/c} dz$ and $V_{b2} = \int_{b2} E_z e^{i\omega_0 z/c} dz$ respectively. By Ohms law it can then be seen that

$$\begin{pmatrix} V_{b1} \\ V_{b2} \end{pmatrix} = \begin{bmatrix} Z_{11} & Z_{12} \\ Z_{21} & Z_{22} \end{bmatrix} \begin{pmatrix} I_{b1} \\ I_{b2} \end{pmatrix}. \tag{21}$$

The power loss due to both beams can then be seen to be

$$P_{loss} = \begin{pmatrix} V_{b1} & V_{b2} \end{pmatrix} \begin{pmatrix} I_{b1} \\ I_{b2} \end{pmatrix}^*. \tag{22}$$

In the worst case scenario, the values of the impedance matrix are real, and are equal in value to the peak values of the resonant impedance

$$Z_{11} = 2R_s^{b1};\ Z_{22} = 2R_s^{b2};\ Z_{12} = Z_{21} = 2\sqrt{R_s^{b1} R_s^{b2}}. \tag{23}$$

The power loss then becomes

$$P_{loss} = I_0^2 2 \left(R_s^{b1} + R_s^{b1} - 2\sqrt{R_s^{b1} R_s^{b2}} cos\left(\delta\phi\right) \right) \tag{24}$$

where $\delta\phi = \phi_1 - \phi_2$ is the phase difference between beam 1 and beam 2. This can be found relatively easy by comparing the distance δs from a collision IP of the machine. Assuming the beams are ultrarelativistic $\delta\phi = \omega_{rev} 2\delta s/c$. It can then be seen that the the last term may either reduce or increase the power loss depending on whether $cos\left(\delta\phi\right) = 1$ or $cos\left(\delta\phi\right) = -1$ respectively.

0.7 Summary

In this note we have presented an in depth derivation of the origin of beam induced heating and how to calculate the impedance for a variety of types of impedance. An emphasis has been placed on correctly understanding the effects of changing beam parameters on the power loss due to impedances, in particular the longitudinal bunch distribution. It has been seen that the choice of distribution can greatly change the power loss, especially due to high frequency lobes which have been observed in many machines. In addition the power loss due to two beams in the same vacuum chamber has been briefly covered to illustrate some of the more niche problems that can occur in accelerator design.

0.8 Appendix

0.8.1 Bunch Profiles in the Frequency Domain